Article:
Hubbard, CG, West, LJ orcid.org/0000-0002-3441-0433, Rodriguez-Blanco, JD et al. (1 more author) (2014) Laboratory study of spectral induced polarization responses of magnetite - Fe2+ redox reactions in porous media. Geophysics, 79 (1). 17JF-Z24. ISSN 0016-8033

https://doi.org/10.1190/GEO2013-0079.1

Laboratory Study of Spectral Induced Polarization Responses of Magnetite - Fe^{2+} Redox Reactions in Porous Media

Christopher G. Hubbard[1,2], L. Jared West[1*], Juan Diego Rodriguez-Blanco[1,4] and Samuel Shaw[1,3]

[1]School of Earth and Environment, University of Leeds, Leeds, UK

[2]Now at Earth Sciences Division, Lawrence Berkeley National Laboratory, Berkeley, CA, USA, cghubbard@lbl.gov

[3]Now at School of Earth, Atmospheric and Environmental Science, University of Manchester, UK, sam.shaw@manchester.ac.uk

[4]Now at Nano-Science Center, University of Copenhagen, Denmark, jblanco@nano.ku.dk

*Corresponding author: L.J.West@leeds.ac.uk

Right Running Head: **SIP of Magnetite-Fe^{2+} Redox Reactions**

Date of Submission: 27th February 2013

ABSTRACT

Spectral Induced Polarization (SIP) phase anomalies in field surveys at contaminated sites have previously been shown to correlate with the occurrence of chemically reducing conditions and/or semiconductive minerals, but the reasons for this are not fully understood. We report a systematic laboratory investigation of the role of the semiconductive mineral magnetite and its interaction with redox-active versus redox-inactive ions in producing such phase anomalies. The SIP responses of quartz sand with 5% magnetite in solutions containing redox-inactive Ca^{2+}, and Ni^{2+}, versus redox-active Fe^{2+} were measured across the pH ranges corresponding to adsorption of these metals to magnetite. With redox inactive ions Ca^{2+} and Ni^{2+}, SIP phase response showed no changes across the pH range 4 to10, corresponding to their adsorption, showing ~30 mrad anomalies peaking at ~59 to 74 Hz. These large phase anomalies are probably caused by polarization of the magnetite-solution interfaces. With the redox-active ion Fe^{2+}, frequency of peak phase response decreased progressively from ~46 to ~3 Hz as effluent pH increased from 4 to 7, corresponding to progressive adsorption of Fe^{2+} to the magnetite surface. The latter frequency (3 Hz) corresponds approximately with those of phase anomalies detected in field surveys reported elsewhere. We conclude that pH sensitivity arises from redox reactions between Fe^{2+} and magnetite surfaces, with transfer of electrical charge through the bulk mineral, as reported in other laboratory investigations. Our results confirm that SIP measurements are sensitive to redox reactions involving charge transfers between adsorbed ions and semiconductive minerals. Phase anomalies seen in field surveys of groundwater contamination and biostimulation may therefore be indicative of iron-reducing conditions, when semiconductive iron minerals such as magnetite are present.

INTRODUCTION

Geophysical approaches are proving increasingly useful for monitoring changes in subsurface geochemistry. Over recent decades, non-invasive geophysical techniques that can be used from the ground surface such as resistivity, (spectral) induced polarization (SIP), electromagnetic and self-potential surveys have been developed for locating and characterizing contaminant plumes (Sauk et al., 1998; Naudet et al., 2003) and monitoring in-situ remediation schemes (Hubbard et al., 2008; Atekwana and Slater, 2009). This is particularly relevant to some nuclear legacy sites such as areas of Hanford (Washington), Oak Ridge (Tennessee), and Rifle (Colorado) in the USA and Sellafield in the UK (Hunter, 2004; Catalano et al., 2006; Kelly et al., 2008; Williams et al., 2009), where invasive surveys may be very difficult due to radiotoxicity of contaminant plumes and the possibility of compromising the hydraulic integrity of the subsurface. The need for monitoring subsurface geochemistry such as redox conditions at contaminated sites has been recognized, because they play a vital role in controlling the mobility of key redox-active contaminants such as Cr, U, Tc and As (Finneran et al., 2002; Islam et al., 2004; Burke et al., 2005; Hubbard et al., 2008). Thus, remote sensing of redox indicators, such as the presence of Fe(II) in groundwater or the formation of sulfide minerals (Ntarlagiannis et al., 2005, 2010a; Personna et al., 2008), would be a highly valuable complementary approach to conventional sampling and geochemical analysis of groundwater.

An example of non-invasive monitoring of subsurface geochemical redox-state and hence contaminant mobility at a radionuclide contaminated site via complex resistivity/induced polarization was undertaken at the Rifle site in Colorado, USA. Here, acetate was injected into groundwater to create (bio)reducing conditions for uranium immobilization (Williams et al., 2009; Flores Orozco et al., 2011; Chen et al., 2012). Flores Orozco et al. (2011) correlated the largest phase anomalies seen at the site (~40 mrad) with geochemical conditions where aqueous Fe(II) was present in the pore fluid at locations that had previously undergone sulfate reduction. They concluded that these large phase signals arose from the interaction of electroactive Fe(II) and semiconductive sulfide minerals (e.g. pyrite, FeS_2). Another semiconductive mineral phase, detrital magnetite (Fe_3O_4), has also been reported in the Rifle sediment (Campbell et al., 2012). The importance of magnetite in geophysical investigations of contaminated sites has been highlighted by recent surveys at the Bemidji site (Minnesota, USA). Here geophysical

anomalies are spatially correlated with the presence of magnetite located in the zone of water table fluctuation above a degrading hydrocarbon plume originating from a crude oil spill (Mewafy et al., 2011).

In this study, we follow-up on the field results outlined in the previous paragraph by performing a systematic laboratory investigation of the spectral induced polarization (SIP) responses of dispersed semiconductive mineral particles – in this case magnetite – with both redox active (Fe^{2+}) and inactive (Ca^{2+} and Ni^{2+}) ions and pH. The rationale for our study lies in the need to better constrain the fundamental mechanisms responsible for the large phase responses associated with dispersed semiconductive minerals and the degree of dependence of these responses on the geochemical conditions (e.g. pH). It is believed that SIP phase responses for semiconductive particles arise both because the particles themselves polarize strongly, owing to high mobility of charges within them, but also from redox reactions at semiconductive particle surfaces that allow charge transfer to and from the pore fluid (Wong, 1979; Slater et al., 2005; Wu et al., 2005; Slater et al., 2006; Williams et al., 2009; Ntarlagiannis et al., 2010a,b). Ambiguity in the interpretation of SIP phase responses arises partly from the difficulty in distinguishing between these mechanisms. In this laboratory study, we use chemical control on surface electrochemical reactions in order to identify the origin of the SIP responses for magnetite in various geochemical conditions. Our study takes advantage of the pH dependence of surface redox reactions between Fe^{2+} and Fe (oxyhydr)oxides such as magnetite to distinguish between possible mechanisms. These reactions can only occur where adsorption of Fe^{2+} allows sufficient proximity to the mineral surface. Before outlining the methodology and presenting the results of this study, we therefore first review current knowledge of (i) magnetite electron transfer and surface charge, (ii) SIP response of (semi)conductive particles.

Magnetite mobile charges, surface properties and redox reactions

Magnetite (Fe_3O_4) is a spinel group mixed ferrous-ferric iron oxide mineral formed in a wide variety of environments, from low-temperature near-surface to hydrothermal conditions. It is an n and p type small band gap semiconductor at room temperature with the highest electrical conductivity of any oxide, of 1 – 10 $\Omega^{-1}m^{-1}$ (Cornell and Schwertmann, 2003). Mobile charges within the magnetite lattice may be either electron or hole polarons situated on lattice sites occupied by Fe atoms, which migrate by

electron hopping (Tsuda et al., 2000; Skomurski et al., 2010), or mobile Fe^{2+} ions hopping between unoccupied lattice sites (Gorski et al., 2012). The rapid movement of such charges within the magnetite lattice gives rise to its high electrical conductivity (Skomurski et al., 2010; Gorski et al., 2012).

The magnetite-solution interface is terminated by iron oxide and hydroxyl groups (e.g. $>FeOH_2^{+1/2}$) with pH-dependent charge, and can be represented most simply with a 1-pK protonation model (Wesolowski et al., 2000). As pH increases from below the point of zero charge (pzc) for magnetite (pH 6.3-7.1; Marmier et al., 1999) to above it, the $>FeOH_2^{+1/2}$ surface functional groups become progressively deprotonated to $>FeOH^{-1/2}$ and the net surface charge changes from positive to negative. The adsorption of metal ions (such as Ca^{2+}, Ni^{2+} and Fe^{2+} used in our study) to the surface of magnetite is also controlled by pH. At pH ~4 Ca^{2+}, Ni^{2+} and Fe^{2+} ions do not adsorb to the mineral surface. With increasing pH, metal ion adsorption increases until the limit of surface adsorption is reached. This zone of increasing adsorption ('the adsorption edge') often occurs over a narrow pH range, with the range varying according to the metal ion, solution composition and the mineral substrate. Both Ni^{2+} and Fe^{2+} adsorb to the surface of magnetite via inner sphere complexes, with increasing adsorption over the pH range 5 to 8 (Marmier et al., 1999; Vikesland and Valentine, 2002), whereas Ca^{2+} adsorption to iron (oxyhydr)oxides has been modeled via both inner and outer sphere complexation, with the adsorption edge near or above the mineral pzc (Rahnemaie et al., 2006).

Charge transfers from adsorbed redox-active ions such as Fe^{2+} to semiconductive iron minerals have been observed in abiotic laboratory studies. Yanina and Rosso (2008) observed a chemically induced electrical potential gradient between different faces of hematite (α-Fe_2O_3) crystals in solutions containing Fe(II). This potential resulted in electron transfer reactions between adsorbed Fe(II) and Fe(III) within the hematite structure, inducing current flow through the crystal, involving conversion of adsorbed Fe^{2+} to lattice-bound Fe^{3+} on the 001 crystal face and corresponding dissolution of hematite to form aqueous Fe^{2+} on the hk0 crystal face, with electron transfer via semiconductive hematite, i.e.,

$$Fe^{2+}_{(ads)} \rightarrow Fe^{3+}_{(s)} + e^-, \quad (1)$$

$$Fe^{3+}_{(s)} + e^- \rightarrow Fe^{2+}_{(aq)}, \quad (2)$$

Near-complete isotopic exchange between $^{57}Fe^{2+}_{(aq)}$ and bulk goethite (α-FeOOH) was observed at pH 7.5 by Handler et al. (2009). They proposed a mechanism of $Fe^{2+}_{(aq)}$ adsorption, electron transfer through

the bulk mineral and simultaneous mineral growth and dissolution on separate crystal faces, similar to that proposed by Yanina and Rosso (2008) for hematite. Gorski et al. (2012) used a similar isotopic approach to investigate magnetite surface reactions. They confirmed isotopic exchange between aqueous Fe^{2+} and magnetite at ~pH 6.0, which is consistent with surface redox reactions such as (1) and (2) above.

The abovementioned studies indicate that, due to the ubiquitous nature of iron (oxyhydr)oxide semiconductors such as magnetite, charge transfers between aqueous Fe^{2+} and these minerals are likely to be common within anaerobic subsurface environments. The documented ability of the SIP technique to detect such semiconductive minerals and the potential for SIP to also detect charge transfer reactions at these mineral surfaces (Marshall and Madden, 1959; Wong et al, 1979) is therefore of great practical significance. SIP responses are briefly reviewed in more detail in the following section.

Spectral induced polarization response of (semi)conductive particles

Spectral Induced Polarization (SIP) measures impedance magnitude and phase response over a range of frequencies, typically 0.1 to 1000 Hz. In field surveys, practical considerations such as electromagnetic coupling have historically limited the maximum frequency that could be measured to <10 Hz (Williams et al., 2009), although efforts are currently being made to extend this range to higher frequencies through improved instrumentation and methods for removing high-frequency noise (e.g. Ingeman-Nielsen and Baumgartner 2006; Ghorbani et al., 2009). SIP impedance magnitude depends mainly on the d.c. electrical conductivity, which is in turn dependent on the electrolytic conductivity of the fluid in interconnected fluid-filled pores and electrical double layer (EDL), provided that any conductive or semiconductive minerals present do not form continuous current pathways. Like traditional IP current-decay times, SIP phase responses are related to polarization phenomena, i.e. movement of electrical charges that are spatially limited, for example due to polarization of interfaces between minerals and pore solution (Wong, 1979; Vaudelet et al., 2011).

SIP phase responses have been attributed to several different types of polarization phenomena including those associated with microbial cells and biofilms (Davis et al., 2006), non-conductive minerals such as silica (Vaudelet et al., 2011; Zhang et al., 2012), and (semi)conductive particles such as sulfides

(Ntarlagiannis et al., 2005, 2010a, 2010b), magnetite and Fe(0) particles (Slater et al., 2005). Microbes and biofilms produce relatively small phase responses of typically <2 mrad (Ntarlagiannis and Ferguson, 2009). Detection of such responses in field surveys is likely to be very difficult. Non-conductive minerals also typically produce small SIP phase responses arising from ion migration within the electrical double layer (EDL) at the mineral-water interface (typically <<10 mrad at frequencies <1000 Hz; Vaudelet et al., 2011; Zhang et al., 2012). In contrast, semiconductive minerals dispersed in a matrix of non-conducting minerals, including natural authigenic minerals such as magnetite, secondary precipitates and metallic particles may give larger phase responses, typically of the order of several tens to hundreds of mrad (Slater et al., 2005; Personna et al, 2008; Ntarlagiannis et al., 2010a). These strong polarization responses associated with semiconductive minerals have been interpreted in terms of two phenomena:

(i) polarization of the interface between the semiconductive particle and the pore fluid, facilitated by movement of mobile charges within the semiconductive mineral particles, balanced by build-up of oppositely charged ions in the pore fluid adjacent to the particle surface and

(ii) electrochemical redox reactions at the particle surface which allow charge to be transferred across these interfaces (for example such as reactions (1) and (2) above).

Mechanism (i) is supported by the dependence of the peak phase frequency on semiconductive mineral particle size, with peak frequency reducing as polarizable particle size increases (Pelton et al., 1978; Wong, 1979; Olhoeft, 1985). For mechanism (ii), Wong (1979) modeled the occurrence of electrochemical reactions at the interface between semiconductive minerals and the pore fluid, and showed that such reactions will reduce the frequency of the peak phase response.

Recent laboratory investigations of such large SIP phase responses have focused specifically on those associated with biostimulation efforts. They found secondary minerals such as sulfide precipitates produced phase anomalies of up to 60 mrad associated with both abiotic and microbial precipitation of iron and zinc sulfides (Ntarlagiannis et al., 2005, 2010a, 2010b; Williams et al., 2005; Slater et al., 2007; Personna et al., 2008). Laboratory experiments on sediments from the biostimulation field site at Rifle, CO, agreed with field results suggesting that redox-active ions may play an important role in the observed SIP signals (Williams et al., 2009) but highlighted that more controlled experiments were needed (Ntarlagiannis et al., 2010b). In this study we therefore sought to clarify the role of pore fluid pH, Fe^{2+}

adsorption and associated surface redox reactions with semiconductive Fe-minerals, such as (1) and (2) above, in the generation of SIP phase anomalies.

METHODS

Two separate experiments were conducted on 5 wt% magnetite - 95 wt% sand mixtures using the apparatus illustrated in Figure 1. The aim of experiment A was to compare the SIP response for redox-inactive Ca^{2+} with redox-active Fe^{2+}, as pH was adjusted from ~4 where all the metal ions were in solution to between 7 and 10, thereby resulting in progressive adsorption of each metal to the surface of magnetite (Cornell and Schwertmann, 2003). Experiment B was conducted in a similar fashion on a separately packed magnetite-sand mixture using solutions of $CaCl_2$ and $NiCl_2$. The objective of this subsequent experiment was to measure the SIP response for a cation (Ni^{2+}) with similar inner-sphere adsorption behavior to Fe^{2+} but which is redox-inactive. The use of $CaCl_2$ in experiment B was to repeat the first phase of experiment A on a separately packed but otherwise identical magnetite-sand mixture. This allowed the effects of any variations in specimen packing to be identified and distinguished from those of fluid chemistry.

The sample holder used was similar to previously published cells (e.g. Vinegar and Waxman, 1984; Binley et al., 2005), consisting of a vertically-oriented cylinder (length = 5 cm, diameter = 3 cm), with Ag-AgCl ring electrodes for current injection, mounted in fluid-filled end caps above and below the sample (Figure 1). Ag-AgCl potential electrodes were mounted in fluid-filled side chambers attached to these end-caps, such that the potential electrodes did not protrude into the current pathway. Rubber o-rings were located between the sample holder and end-packs, and valves were fitted at the influent and effluent ports. This allowed for testing of the sample holder to ensure it was air-tight in order to prevent sample oxidation during the experiments. As an extra precaution, we used PFA and PVC tubing with low gas permeability. Solutions of 2.5 mM redox-active $FeCl_2$ and redox-inactive $CaCl_2$ and $NiCl_2$ were prepared using deoxygenated water. These solutions were constantly purged with N_2 to keep them anaerobic throughout the experiment – ferrous iron analyses (Fe^{2+} = 2.53 ± 0.08 mM, mean ± 1σ, n=12) showed that this was sufficient to maintain reduced conditions. Solutions were constantly recirculated upwards through the vertically-oriented sample column, from a 2 L reservoir at 24 mL/min (2 pore

volumes/min), as shown in Figure 1. The samples themselves consisted of a mix of 5 wt% magnetite (Excalibur Mineral Corp., NY; crushed single crystals sieved to 1-2 mm with a flaky and angular morphology) and 95 wt% Ottawa sand (Fisher Scientific; 590–840 μm, well rounded quartz sand), mixed together when dry before being wet packed into the sample holder with regular gentle tapping to ensure packing homogeneity. Sample porosity was ~0.35, determined from the weight of mix used, mineral specific gravities (2.65 g cm^{-3} for quartz; 5.15 g cm^{-3} for magnetite) and sample holder dimensions.

Spectral induced polarization (SIP) measurements of the impedance magnitude and phase response of the sample were made relative to a reference resistor using a National Instruments 4461 Dynamic Signal Analyzer at 40 logarithmic intervals from 0.1 to 1000 Hz (Ntarlagiannis et al., 2005) and corrected for the geometry of the sample holder. Capacitive coupling effects at high frequencies in this set-up are associated with both (i) the reference resistor and (ii) the sample holder components of the circuit; these were minimized by first performing calibrations with solutions of known conductivity that allowed the reference resistor to be set at a value such that (i) and (ii) cancelled out.

In detail, the sample for experiment A was first packed and saturated with 2.5 mM $CaCl_2$ that had been adjusted to pH 4.5 with HCl. After measuring the SIP response as described in the previous paragraph, pH was adjusted sequentially up to pH ~10 in the solution reservoir using small volumes of NaOH and HCl (1, 10 and 100 mM as needed, to a maximum concentration of 0.6 mM Na^+ in the final solution). SIP response was measured after each pH increment. The sample was then flushed through with >50 pore volumes of 2.5 mM $FeCl_2$ at pH ~4, to thoroughly exchange the pore fluid and allow for calcium desorption (pH 4 is below the adsorption edge for Ca^{2+} adsorption onto iron (oxyhydr)oxides; Rahnemaie et al., 2006). The $FeCl_2$ solution was then allowed to recirculate through the sample and the influent reservoir (Figure 1), where pH was increased sequentially up to pH ~8 with NaOH and the SIP response was measured at each pH increment. Experiment B was subsequently conducted in a similar fashion on a separately packed 5 wt% magnetite - 95 wt% sand mixture using solutions of (i) 2.5 mM $CaCl_2$ and (ii) 2.5 mM $NiCl_2$. After adjusting the pH in the influent reservoir, the solution was typically recirculated for ~100 pore volumes before measuring the SIP response together with the influent and effluent pH, fluid conductivity and temperature. In total, 5 - 6 measurements were taken across the pH range for $CaCl_2$ and $NiCl_2$ solutions, whereas 13 measurements were taken for the $FeCl_2$ solution as the

SIP response showed greater variation. Note that the final 5 $FeCl_2$ measurements for $FeCl_2$ were replicates of the pH trend, to test for reproducibility of the phase response – the influent pH was reduced down to ~5 before being increased sequentially up to pH ~8. For the $FeCl_2$ experiment, Fe^{2+} analyses of influent and effluent samples were also performed following the spectrophotometric method of Stookey (1970). The pH was not adjusted to below 4 or above 10 as this would significantly change the fluid conductivity of the solution; maintaining fluid conductivity approximately constant facilitates interpretation of SIP phase responses (Slater et al., 2005). Note that the maximum pH in the experiments with Fe^{2+} and Ni^{2+} was constrained to ~pH 7 to 8 by the solubility of their hydroxides: modeling using the PHREEQC geochemical speciation code (Parkhurst, 1995) indicated that the metal hydroxide would precipitate at higher pH.

Phenomenological models are often used to describe SIP data; we use a single dispersion Cole-Cole model (Cole and Cole, 1941; Pelton et al., 1978) as outlined below in equation (3), where $\rho^*(\omega)$ is the complex resistivity (Ωm) at angular frequency ω, ρ_0 is the DC resistivity (Ωm), m is the chargeability (dimensionless), i is $\sqrt{-1}$, τ is the mean relaxation time (secs), and c is a shape exponent (dimensionless). SIP data are inverted with the Bayesian model of Chen et al. (2008) using Markov-chain Monte Carlo sampling methods.

$$\rho^*(\omega) = \rho_0 \left\{1 - m\left[1 - \frac{1}{1 + (i\omega\tau)^c}\right]\right\} \qquad (3)$$

The attraction of this modeling approach is that it can simply capture the frequency-dependence of the conduction and charge storage/polarization characteristics. The limitations are that it is inherently non-mechanistic and that the derived parameters are interdependent. Previous investigators have therefore normalized Cole-Cole parameters to account for this interdependence (e.g. $m_n = m / \rho_0$; $\tau_n = \tau / \rho_0$) and have attempted to systematically relate changes in these parameters with variations in physical and chemical properties. For example, Slater et al. (2005, 2006) showed linear relationships between m_n and polarizable surface area per unit pore volume for magnetite and zero-valent iron particles dispersed in a sand matrix. Multiple studies (Pelton et al., 1978; Wong, 1979; Olhoeft, 1985; Slater et al., 2005) have also highlighted how relaxation time is controlled by both the polarizable mineral size and the solution ionic strength – note that these are two parameters which we have kept invariant in this study. We present both basic and normalized Cole-Cole parameters to enable comparison with previous studies.

RESULTS

The spectral induced polarization data from our 5 wt% magnetite in quartz sand experiments are shown in Figure 2. The graphs show the data for three different pore fluids: 2.5 mM $CaCl_2$ (Figure 2 a,b), 2.5 mM $NiCl_2$ (Figure 2c,d) and 2.5 mM $FeCl_2$ (Figure 2e,f) from the two different experiments (A and B) conducted on separately packed magnetite-sand mixtures as outlined in the methods section. The three graphs on the left hand side (Figure 2a,c,e) show the phase response (mrad) as a function of frequency (Hz) and pH, while the three graphs on the right hand side (Figure 2b,d,f) show the measured resistivity magnitude (Ωm). Note that the resistivity axis has been greatly expanded to highlight the frequency-dependence; with the exception of one sample (the highest pH sample [pH 9.9] for $CaCl_2$ in experiment A, with the greatest NaOH addition), all resistivity magnitude and fluid conductivity measurements show less than 4% deviation from the start of each pH manipulation. These small fluid conductivity (and resistivity magnitude) changes with pH largely reflect the addition of acid/base. Figure 2a shows that experiment A exhibited very little variation in phase response over effluent pH 4.5 - 9.9 with $CaCl_2$ pore fluid, with a peak phase of 30.0 ± 0.3 mrad (mean ± 1σ, n=5) at 59-74 Hz. The repeat with $CaCl_2$ pore fluid in experiment B (a separate magnetite-sand mix) showed good reproducibility when compared with experiment A, with a similar peak phase of 31.9 ± 0.3 mrad (mean ± 1σ, n=6) at 59 Hz (Figure 2a). The minor variations in response between specimens A and B with $CaCl_2$ pore fluid are believed to arise from slight variations in packing of the sand-magnetite mix. The resistivity response (Figure 2b) was also similar for both experiments ($CaCl_2$ (A) = 77.2 ± 1.8 Ωm at 0.1 Hz; $CaCl_2$ (B) = 80.5 ± 0.4 Ωm at 0.1 Hz), with a characteristic decrease of ~7 % from 0.1 Hz to 1000 Hz and steepest gradient (i.e. inflection point) at the frequency of the peak phase response. $NiCl_2$ pore fluid experiment gave the same phase response as $CaCl_2$ (specimen B, Figure 2c), with a phase peak of 31.7 ± 0.4 mrad (mean ± 1σ, n=6) at 59 Hz over pH 4.3 - 7.4; resistivity (Figure 2d) was slightly higher (84.6 ± 0.8 Ωm) because the fluid conductivity was slightly lower (535 ± 5 µS/cm at 19.7 ± 0.1 ºC) than with $CaCl_2$ pore fluid (567 ± 5 µS/cm at 19.9 ± 0.1 ºC).

For $FeCl_2$ pore fluid, the frequency of the peak phase was highly dependent on effluent pH, decreasing from 46 Hz at pH 4.0, to 16 Hz at pH 5.8 and 2.7 Hz at pH 7.0 (Figure 2e). The peak phase magnitude was slightly smaller and also showed more variability than in the $CaCl_2$ and $NiCl_2$ experiments,

ranging from 28.4 mrad at pH 4.0, to 24.6 mrad at pH 6.3 and 25.8 mrad at pH 7.0. The resistivity (79.8 ± 1.1 Ωm at 0.1 Hz; Figure 2f) and the fluid conductivity (581 ± 3 μS/cm at 22.1 ± 0.6 ºC) showed only minor variations with pH; the inflection point in the frequency dependent resistivity response varied systematically with pH, as expected from the variation in phase response.

Figure 3 shows the frequency of the peak phase versus effluent pH for all pore fluids, highlighting minimal variation with pH for $CaCl_2$ and $NiCl_2$ but decreasing peak frequency for $FeCl_2$ as effluent pH increases from 4 to 7. Note that peak frequencies of the replicate $FeCl_2$ data points are coincident with those from the initial experiment indicating that the change in frequency with pH in this system is reproducible. A range of published adsorption curves for Fe^{2+} on iron (oxyhydr)oxides, including magnetite, are also shown for comparison (Vikesland and Valentine, 2002 and references therein). It can be seen that in the $FeCl_2$ experiment, the peak phase frequency reduces over a similar pH range to which Fe^{2+} adsorption to iron (oxyhydr)oxide phases occurs. This shows that as the amount of Fe^{2+} adsorbed to the surface of the magnetite increases (pH 4 to 7), the peak phase frequency decreases. However, based on the quantity of magnetite relative to the concentration and volume of dissolved Fe^{2+} used in our experiments, the total proportion of adsorbed Fe^{2+} in our experiments is likely to be small relative to the $Fe^{2+}_{(aq)}$ concentration in solution, indicating that the ionic strength of the solution will remain relatively constant throughout. Note that, effluent pH was below that of the influent, most noticeably in the $FeCl_2$ experiment, especially at circumneutral pH (see horizontal 'error' bars in Figure 3). The solutions used in this experiment were unbuffered and N_2-purged in order to keep data interpretation as simple as possible, so any net release of even μM concentrations of protons (e.g. by metal adsorption) will have reduced pH (the flow-rate of the experiments was kept high to try and minimize this effect). Despite significant pH variations between influent and effluent as shown in Figure 3, it is clear that the change in peak phase frequency for the $FeCl_2$ pore fluid occurred over the pH range corresponding to progressive Fe^{2+} adsorption to magnetite. No similar trend was observed for redox-inactive ions Ca^{2+} and Ni^{2+} despite the fact that the adsorption of these ions to the magnetite surface increases from zero to maximum surface coverage over the measured pH range (Marmier et al, 1999; Rahnemaie et al., 2006).

Cole-Cole modeling shows reasonable fits to the data (Figure 4). Note that modeling was performed for the frequency range 0.1 to 94 Hz as this gave the best fits to the position of the phase peak

for the $FeCl_2$ data i.e. the measured parameter that varied most significantly in this study. Consequently, the greatest deviation between modeled and measured data is seen when extrapolating this fit to frequencies >94 Hz (dashed lines, Figure 4). This is the frequency range where instrument errors (capacitive coupling) commonly become most significant for the instrument used in this study, despite efforts for error minimization (e.g. Binley et al., 2005). Table 1 summarizes the Cole-Cole data – it can clearly be seen that (i) the $FeCl_2$ data shows the most variation, and (ii) the time constants τ and τ_n are the parameters that change the most with pH, showing a 17x increase as (effluent) pH increases from 4 to 7. A comparison with previous studies highlights that Slater et al (2005) also showed an approximately 10-20x increase in normalized relaxation time (τ_n) when pH was increased from 3 to 10.5 for experiments with 5 % zero-valent iron dispersed in a sand matrix, although their experiments were not designed to investigate the mechanisms behind this. Furthermore, normalized chargeability values (m_n) in our study are similar to those reported by Slater et al. (2005, 2006) for low percentage mixtures of magnetite or zero-valent iron with sand. Indeed, the 5 % magnetite sample (mean radius = 0.43 mm) of Slater et al. (2006) gives a m_n value of ~3 mS/m, compared with ~1 mS/m in our study. However, as has been noted previously in multiple studies (e.g. Slater et al., 2005; Zhang et al., 2012), Cole-Cole parameters suffer from non-uniqueness, may be correlated and their physical significance is unknown. We therefore prefer to focus on the measured parameters (resistivity magnitude, phase shift and the frequency of peak phase shift) in our following discussion of the data.

DISCUSSION

Our results illustrate that SIP measurements are sensitive to the adsorption of the redox-active ion Fe^{2+} on magnetite, but insensitive to the adsorption of redox-inactive ions Ni^{2+} and Ca^{2+}. We observed a strong correlation between peak phase frequency and pH and hence by inference the amount of Fe^{2+} adsorption to magnetite, which increases across the pH range of 5 to 7 (Figure 3). No such correlation was observed for redox-inactive species Ca^{2+} and Ni^{2+} despite the fact that they also adsorb to the magnetite surface over the measured pH range. We note that Ca^{2+}, Ni^{2+}, and Fe^{2+} will also have adsorbed to the surface of silica grains within our samples - however, the phase responses associated with silica grains are typically very much smaller than those seen in our study (e.g. Leroy et al., 2008;

Zhang et al., 2012), which we thus attribute to the semiconductive magnetite particles. An interpretation of our data based on the responses of magnetite particles is illustrated by the conceptual model shown in Figure 5. At pH ~4 (Figure 5a) the magnetite surface is positively charged owing to protonation of surface iron hydroxyl groups, therefore the electrical double layer (EDL) consists mainly of negatively charged ions. Most metals ions Me^{2+} including Ca^{2+}, Ni^{2+} or Fe^{2+}, do not interact with the magnetite surface at this pH (Langmuir, 1997). The application of electric field E during SIP measurement creates a polarized interface at the magnetite surface owing to migration of mobile charges within the magnetite lattice, and corresponding build-up of counter-ions in the adjacent pore solution; however, because there is no adsorption of redox-active ions, no charge can be transferred across this interface. Note that interface polarization will be in opposite directions at opposite ends of the magnetite particle, as shown in Figure 5a.

Under the applied electrical field, charge builds up on either side of each interface (ions in the pore solution and electronic charges in the magnetite) until electrostatic repulsion between like charge carriers prevents further accumulation (Wong, 1979). The characteristic charging (or relaxation) time and hence frequency of the peak phase response depends on the ionic strength of the pore solution (Slater et al., 2005), with more dilute solutions producing longer characteristic times and hence lower peak frequencies; this is because interface charging takes longer when there are fewer ions in the pore solution. In our experiments, the large ~30 mrad magnitude polarizations with peak frequencies at ~59 – 74 Hz are thought to have arisen from this mechanism; these are seen for Ca^{2+} and Ni^{2+} ions across the pH range tested. Similarly, the ~46 Hz peak response for Fe^{2+} ions at pH <5 is thought to arisen from this mechanism, because at this pH the interaction of Fe^{2+} with the magnetite surface is likely to be minimal. The fact that the peak response frequencies seen for Ca^{2+} and Ni^{2+} are insensitive to pH (see Figures 2 and 3) suggests that the polarization mechanism is insensitive to the surface charge on magnetite, which will reverse across the pH range tested. We therefore infer that under an applied electrical field, the polarization contribution due to the migration of mobile charges within the magnetite particle itself dominates over the contribution from magnetite surface hydroxyl groups. This essentially alters the distribution and quantity of charged ions within the EDL to balance the polarized mobile charges in the magnetite, rather than the charged surface hydroxyl groups. We propose that this hypothesis could be

tested by measuring the SIP response of different iron (oxyhydr)oxide minerals e.g. hematite and goethite, as both have similar surface functional groups to magnetite that exhibit similar changes in protonation with pH. However, hematite is much more conductive than goethite, so whereas hematite is likely to exhibit similar SIP behavior to magnetite, we predict that goethite will have a much smaller phase response that predominantly reflects pH-dependent surface charge from iron hydroxyl groups, rather than the migration of mobile charges within the mineral itself. This dominant SIP polarization mechanism (related to polarization of an EDL defined by pH-dependent surface charge) has previously been demonstrated by Skold et al. (2011) for silica. We also note that surface charges might however be more important in field SIP measurements, where smaller iron (oxyhydr)oxide mineral particles and smaller applied voltage gradients than those used in this study may be present.

Between pH 5 – 8 the magnetite passes through its pzc (at pH 6.3 – 7.1); the magnetite surface has both positively and negatively charged hydroxyl groups and becomes progressively more negative as pH increases above the pzc. The adsorption of Ca^{2+}, Ni^{2+} and Fe^{2+} to the magnetite surface progressively increases across this pH range (Vikesland and Valetine, 2002),. In the case of Fe^{2+}, previous work on iron (oxyhydr)oxides including magnetite (Yanina and Rosso, 2008; Handler et al., 2009; Gorski et al., 2012) suggests that provided Fe^{2+} can interact with the mineral surface, charge transfer can occur to the mineral lattice (see Figure 5b). We therefore infer that the influence of Fe^{2+} adsorption on the phase response is likely to arise from redox reactions or charge transfer between adsorbed Fe^{2+} and magnetite (such as reactions (1) and (2) described previously); the strong sensitivity of the phase peak frequency to increasing pH results from charge transfer via increasing amounts of adsorbed Fe^{2+} ions. The lack of sensitivity to pH for the $CaCl_2$ and $NiCl_2$ experiments arises because there are no corresponding reactions between Ni^{2+} or Ca^{2+} and magnetite. Where charge transfer occurs in the Fe^{2+} case, it must be in opposite directions simultaneously on different faces of the magnetite particle in order to maintain electroneutrality, with growth and dissolution of the particle surface (and in opposite directions on either side of the particle, Figure 5). It may involve conversion of adsorbed Fe^{2+} to lattice-bound Fe^{3+}, and corresponding dissolution of magnetite to form aqueous Fe^{2+}, with electron transfer via semiconductive magnetite. Such a charge transfer mechanism is similar to those observed for hematite in the presence of chemically-induced potential gradients, which resulted in simultaneous growth and dissolution on different

crystal planes (Yanina and Rosso, 2008). The difference here is that the charge transfer is the result of an applied electric field (E) during SIP measurement rather than potential gradients arising from differential adsorption of organic molecules (i.e. oxalate used by Yanina and Rosso, 2008) on different crystal faces. Notably, the redox inactive ions Ca^{2+} and Ni^{2+} will also have progressively adsorbed to the magnetite surface as pH increased, but in these cases there is no corresponding influence on the SIP response (see Figure 3); this suggests that the sensitivity of phase response arises from the redox reaction of Fe^{2+} with magnetite, rather than simply from its adsorption. The occurrence of redox reactions reduces the peak phase frequency (in our experiments to around ~3 Hz at pH ~7); this is consistent with the modeling results of Wong (1979) which show the occurrence of redox reactions at semiconductive mineral surfaces will reduce peak phase frequency, because interfacial charging takes longer where there is leakage of charge across the interface.

It is appropriate to consider the potential implications for interpretation for field scale SIP responses seen at contaminated sites (Williams et al., 2009; Flores Orozco et al., 2011). A key recent result (Flores Orozco et al., 2011) is that the largest phase anomalies seen at the Rifle site (~40 mrad at around ~1 Hz) are seen only where Fe^{2+} is present in the pore fluid in locations that have previously undergone sulfate reduction. Our findings are consistent with their interpretation that this response arises from the interaction between Fe^{2+} and semiconductive minerals present. According to our experimental results, such an interaction is more likely to produce SIP phase responses at the low frequencies (<10 Hz) that were measured in their field surveys. Note that improvements in instrumentation and data processing offer the potential to measure field responses at higher frequencies, so it may now be possible to monitor changes in both phase magnitude and frequency associated with any changes in pH or Fe^{2+} concentration that may occur at a field site containing semiconductive minerals, such as magnetite. Similarly, our results suggest that (S)IP could be used in combination with magnetic susceptibility (Mewafy et al., 2011) to not only prospect for ore minerals and geoarchaeological deposits (e.g. Oldenburg et al., 1997; Florsch et al., 2011) but also to locate subsurface geochemical zones containing both magnetite and pore-water Fe^{2+}, although further work is required to confirm this hypothesis. Further work is also required to confirm whether semiconductive sulfide minerals (rather than magnetite) and other redox-active species can interact to produce similar responses; also whether biogeochemically-

produced nanoparticulate mineral aggregates behave similarly to the highly-crystalline magnetite particles tested here. Modeling simulations of the interaction of the EM field with the magnetite-solution interface, are also desirable in order to confirm that the magnitude and direction of peak frequency changes are consistent with the redox-reaction mechanism proposed, and to investigate how the responses seen in the lab may scale-up to typical field geometries and applied voltages.

CONCLUSIONS

We report a laboratory investigation into the role of redox-active versus redox-inactive ions in generating Spectral Induced Polarization phase anomalies associated with a semiconductive iron mineral (magnetite). This study combines controlled geochemical laboratory experiments with SIP measurements to gain a fundamental understanding of the redox reactions at the mineral/solution interface which control SIP responses, and therefore represents a significant step forward. As has previously been suggested on the basis of field and laboratory studies, our results strongly suggest that interaction between semiconductive minerals such as magnetite and redox-active ions such as Fe^{2+} play a key role in generating such responses; furthermore we identify the key role of pH in controlling such responses. Using mixtures of quartz sand and 5% magnetite, phase anomalies of ~30 mrad peaking at ~59 – 74 Hz were insensitive to pH in the presence of redox-inactive Ca^{2+} and Ni^{2+} ions. As these ions are progressively adsorbed to magnetite as pH increases, we infer that their adsorption does not significantly alter the phase response. In contrast, for Fe^{2+} pore fluid, the frequency of the peak response decreased progressively from ~46 to ~3 Hz as pH was increased from 4 to 7, which we infer corresponds to progressive adsorption of Fe^{2+} to the mineral surface. We suggest from the difference in pH sensitivity here, compared with redox-inactive Ca^{2+} and Ni^{2+} ions, that these changes in response frequency are diagnostic of progressively increasing charge transfer between adsorbed Fe^{2+} and magnetite as adsorption increases; such charge transfers have been confirmed in several previous studies of the surface chemistry of iron (oxyhydr)oxide minerals. We note that the ~3 Hz peak response measured here for the case of redox-reaction with adsorbed Fe^{2+} is similar to low frequency responses detected in recent field surveys where Fe-reducing conditions were present. It thus seems likely that the SIP phase anomalies detected in field surveys of chemically-reducing groundwater are associated with the presence

of Fe^{2+} or other redox-active ions at pH conditions allowing adsorption to semiconductive minerals such as magnetite or sulfides, i.e. the anomalies are suggestive of biogeochemically-induced Fe-reducing subsurface conditions.

ACKNOWLEDGEMENTS

Funding was provided by Royal Society grant RG2010R1 and NERC grant NE/D014026/1. We thank Lee Slater, Dimitrios Ntarlagiannis and Jeff Heenan for assistance in setting-up the SIP equipment; Tony Windross and Rhys Moore for constructing the sample holder; Kath Morris, Dimitrios Ntarlagiannis and Yuxin Wu for their assistance with manuscript preparation, and two reviewers for their insightful comments, which helped improve the manuscript.

REFERENCES

Atekwana, E. A., and L. D. Slater, 2009, Biogeophysics: a new frontier in Earth science research: Reviews of Geophysics, **47**, RG4004.

Binley, A. Slater, L., Fukes, M., and G. Cassiani, 2005, Relationship between spectral induced polarization and hydraulic properties of saturated and unsaturated sandstone: Water Resources Research, **41**, W12417.

Burke, I. T., Boothman, C., Lloyd J. R., Mortimer, R. J. G., Livens, F. R., and K. Morris, 2005, Effects of progressive anoxia on the solubility of technetium in sediments: Environmental Science and Technology, **39**, 4109–4116.

Campbell, K. M., Kukkadapu, R. K., Qafoku, N. P., Peacock, A. D., Lesher, E., Williams, K. H., Bargar, J. R., Wilkins, M. J., Figueroa, L., Ranville, J., Davis, J. A., and P.E. Long, 2012, Geochemical, mineralogical and microbiological characteristics of sediment from a naturally reduced zone in a uranium-contaminated aquifer: Applied Geochemistry, **27**, 1499-1511.

Catalano, J. G., McKinley, J. P., Zachara, J. M., Heald, S. M., Smith, S. C., and G. E. Brown Jr., 2006, Changes in uranium speciation through a depth sequence of contaminated Hanford sediments: Environmental Science and Technology, **40**, 2517–2524.

Chen, J., Kemna, A., and S. S. Hubbard, 2008, A comparison between Gauss-Newton and Markov-chain Monte Carlo–based methods for inverting spectral induced-polarization data for Cole-Cole parameters: GEOPHYSICS, **73**, no. 6, F247–F259.

Chen, J., Hubbard, S., Williams, K., Flores Orozco, A., and A. Kemna, 2012, Estimating the spatiotemporal distribution of geochemical parameters associated with biostimulation using spectral induced polarization data and hierarchical Bayesian models: Water Resources Research, **48**, W05555.

Cole, K. S., and R. H. Cole, 1941, Dispersion and absorption in dielectrics I: Alternating current field: Journal of Chemical Physics, **1**, 341–351.Cornell, R. M., and U. Schwertmann, 2003, The iron oxides: 2nd ed., Wiley-VCH.

Davis C. A., Atekwana, E., Atekwana, E., Slater, L. D., Rossbach, S., and M. R. Mormile, 2006, Microbial growth and biofilm formation in geologic media is detected with complex conductivity measurements: Geophysical Research Letters, **33**, L18403.

Finneran, K. T., Anderson, R. T., Nevin, K. P., and D. R. Lovley, 2002, Potential for bioremediation of uranium-contaminated aquifers with microbial U(VI) reduction: Soil & Sediment Contamination, **11**, 339–357.

Florsch, N., Llubes, M., Téreygeol, F., Ghorbani, A., and P. Roblet, 2011, Quantification of slag heap volumes and masses through the use of induced polarization: application to the Castel-Minier site: Journal of Archaeological Science, **38**, 438-451.

Flores Orozco, A., Williams, K. H., Long, P. E., Hubbard, S. S., and A. Kemna, 2011, Using complex resistivity imaging to infer biogeochemical processes associated with bioremediation of an uranium-contaminated aquifer: Journal of Geophysical Research, **116**, G03001.

Ghorbani, A., Camerlynck, C., and N. Florsch, 2009, CR1Dinv: A Matlab program to invert 1D spectral induced polarization data for the Cole-Cole model including electromagnetic effects: Computers and Geosciences, **35**, 255-266.

Gorski, C. A., Handler, R. M., Beard, B. L., Pasakarnis, T., Johnson, C. M., and M. M. Scherer, 2012, Fe atom exchange between aqueous Fe^{2+} and magnetite: Environmental Science and Technology, **46**, 12399-12407.

Handler, R. M., Beard, B. L., Johnson, C. M., and M. M. Scherer, 2009, Atom exchange between aqueous Fe(II) and goethite: an Fe isotope tracer study: Environmental Science and Technology, **43**, 1102-1107.

Hubbard S. S., Williams, K., Conrad, M. E., Faybishenko, B., Peterson, J. S., Chen, J., Long, P., and T. Hazen, 2008, Geophysical monitoring of hydrological and biogeochemical transformations associated with Cr(VI) biostimulation: Environmental Science and Technology, **42**, 3757–3765.

Hunter, J., 2004, SCLS Phase 1 – Conceptual model of contamination below ground at Sellafield: BNFL Nuclear Sciences and Technology Services Report NSTS 4920.

Ingeman-Nielsen T., and F. Baumgartner, 2006, CR1Dmod: a Matlab program to model 1D complex resistivity effets in electrical and EM surveys: Computers and Geosciences, **32**, 1411-1419

Islam, F.S., Gault, A. G., Boothman, C., Polya, D. A., Charnock, J. M., Chatterjee, D., and J.R. Lloyd, 2004, Role of metal-reducing bacteria in arsenic release from Bengal delta sediments: Nature, **430**, 68-71.

Kelly, S. D., Kemner, K. M., Carley, J., Criddle, C., P. Jardine, M., Marsh, T. L., Phillips, D., Watson, D., and W.-M. Wu, 2008, Speciation of uranium in sediments before and after in situ biostimulation: Environmental Science and Technology, **42**, 1558-1564.

Langmuir D., 1997, Aqueous Environmental Geochemistry: Prentice Hall.

Leroy, P., Revil, A., Kemna, A., Cosenza, P., and A. Ghorbani, 2008, Complex conductivity of water-saturated packs of glass beads: Journal of Colloid and Interface Science, **321**, 103-177.

Marmier, N., Delisee, A., and F. Fromage, 1999, Surface complexation modelling of Yb(III), Ni(II), and Cs(I) sorption on magnetite: Journal of Colloid and Interface Science, **211**, 54-60.

Marshall, D. J., and T. R. Madden, 1959, Induced polarisation, a study of its causes: GEOPHYSICS, **4**, 790-816.

Mewafy, F. M., Atekwana, E. A., Werkema Jr., D. D., Slater, L. D., Ntarlagiannis, D., Revil, A., Skold, M., and G. N. Delin, 2011, Magnetic susceptibility as a proxy for investigating microbially mediated iron reduction: Geophysical Research Letters, **38**, L21402.

Naudet, V., Revil, A., Bottero, J.-Y., and P. Begassat, 2003, Relationship between self-potential (SP) signals and redox conditions in contaminated groundwater: Geophysical Research Letters, **30**, 2091.

Ntarlagiannis D., and A. Ferguson, 2009, SIP response of artificial biofilms: GEOPHYSICS, **74**, A1–A5

Ntarlagiannis, D., Williams, K. H., Slater, L., and S. Hubbard, 2005, Low-frequency electrical response to microbial induced sulphide precipitation: Journal of Geophysical Research, **100**, G02009.

Ntarlagiannis, D., Doherty, R., and K. H. Williams, 2010a, Spectral induced polarization signatures of abiotic FeS precipitation: GEOPHYSICS, **75**, no. 4, F127–F133.

Ntarlagiannis, D., Williams, K., Slater, L., Hubbard, S., and Y. Wu, 2010b, Investigating the effect of electro-active ion concentration on induced polarization signatures arising from biomineral formation: Geochimica et Cosmochimica Acta, **74**, no. 12, A767.

Oldenburg, D. W., Li., Y., and R. G. Ellis, 1997, Inversion of geophysical data over a copper gold porphyry deposit: A case history for Mt. Milligan: GEOPHYSICS, **62**, 1419-1431.

Olhoeft, G. R.,1985, Low-frequency electrical properties: GEOPHYSICS, **50**, 2492-2503.

Parkhurst, D. L., 1995, User's guide to PHREEQC -- a computer program for speciation, reaction-path, advective-transport, and inverse geochemical calculations: U.S. Geological Survey Water-Resources Investigations Report 95-4227.

Pelton, W. H., Ward, S. H., Hallof, P. G., Sill, W. R., and P. H. Nelson, 1978, Mineral discrimination and removal of inductive coupling with multifrequency IP: GEOPHYSICS, **43**, 588-609.

Personna Y. R., Ntarlagiannis, D., Slater, L., Yee, N., O'Brien, M., and S. Hubbard, 2008, Spectral induced polarization and electrodic potential monitoring of microbially mediated iron sulfide transformations: Journal of Geophysical Research Biogeosciences, **113**, G02020.

Rahnemaie, R., Hiemstra, T., and W. H. van Riemsdijk, 2006, Inner- and outer-sphere complexation of ions at the goethite-solution interface: Journal of Colloid and Interface Science, **297**, 379-388.

Sauck W. A., Atekwana, E. A., and M. S. Nash, 1998, High conductivities associated with an LNAPL plume imaged by integrated geophysical techniques: Journal of Environmental and Engineering Geophysics, **2**, 203–212.

Skold, M., Revil, A., and P. Vaudelet, 2011, The pH dependence of spectral induced polarization of silica sands: Experiment and modeling: Geophysical Research Letters, **38**, L12304.

Skomurski, F. N., Kerisit, S., and K. M. Rosso, 2010, Structure, charge distribution and electron hopping dynamics and magnetite (Fe_3O_4) (1 0 0) surfaces from first principle: Geochimica et Cosmochimica Acta, **74**, 4234-4248.

Slater, L. D., Choi, J., and Y. Wu, 2005, Electrical properties of iron-sand columns: implications for induced polarization investigation and performance monitoring of iron-wall barriers: GEOPHYSICS, **70**, no. 4, G87-G94.

Slater, L., Ntarlagiannis, D., and D. Wishart, 2006, On the relationship between induced polarization and surface area in metal-sand and clay-sand mixtures: GEOPHYSICS, **71**, no. 2, A1-A5.

Slater, L., Ntarlagiannis, D., Personna, Y. R., and S. Hubbard, 2007, Pore-scale spectral induced polarization signatures associated with FeS biomineral transformations: Geophysical Research Letters, **34**, L21404.

Stookey, L. L., 1970, Ferrozine - a new spectrophotometric reagent for iron: Analytical Chemistry, **42**, 779-883.

Tsuda, N., Nasu, K., Yanase, A., and K. Siratori, 2000, Electronic Conduction in Oxides: 2nd ed., Springer.

Vaudelet, P., Revil, A., Schmutz, M., Franceschi, M., and P. Begassat, 2011, Changes in induced polarization associated with the sorption of sodium, lead, and zinc on silica sands: Journal of Colloid and Interface Science, **360**, 739-752.

Vikesland, P. J., and R. L. Valentine, 2002, Iron oxide surface-catalysed oxidation of ferrous iron by monochloramine: implications of oxide type and carbonate on reactivity: Environmental Science and Technology, **36**, 512-519.

Vinegar H. J., and M. H. Waxman, 1984, Induced polarisation of shaly sands: GEOPHYSICS, **49**, 1267-1287.

Wesolowski, D. J., Machesky, M. L., Palmer D. A., and L. M. Anovitz, 2000, Magnetite surface charge studies to 290ºC from in situ pH titrations: Chemical Geology, **167**, 193–229.

Williams K. H., Ntarlagiannis, D., Slater, L. D., Dohnalkova, A., Hubbard, S. S., and J. F. Banfield, 2005, Geophysical imaging of stimulated microbial biomineralization: Environmental Science and Technology, **39**, 7592-7600.

Williams, K. H., Kemna, A., Wilkins, M. J., Druhan, J., Arntzen, E. L., N'Guessan, Long, P., Hubbard, S. S., and J. Banfield, 2009, Geophysical monitoring of microbial activity during stimulated subsurface bioremediation: Environmental Science and Technology, **43**, 6717–6723.

Wong, J., 1979, An electrochemical model of the induced polarization phenomenon in disseminated sulfide ores, GEOPHYSICS, 44, 1245–1265.

Wu, Y, Slater, L. D., and N. Korte, 2005, Effect of precipitation on low frequency electrical properties of zerovalent iron columns: Environmental Science and Technology, **39**, 9197-9204.

Yanina S. V., and K. M. Rosso, 2008, Linked reactivity at mineral-water interfaces through bulk crystal conduction: Science, **320**, 218-222.

Zhang, C., Slater, L., Redden, G., Fujita, Y., Johnson, T., and D. Fo, 2012, Spectral induced polarization signatures of hydroxide adsorption and mineral precipitation in porous media: Environmental Science and Technology, **46**, 4357-4364.

LIST OF FIGURES AND TABLES

Figure 1: Schematic of laboratory apparatus (not to scale)

Figure 2: Spectral induced polarization data from 5 % magnetite in quartz sand experiments. a), b) phase and resistivity magnitude respectively for $CaCl_2$ pore fluid in experiments A and B; c), d) $NiCl_2$ and $CaCl_2$ in experiment B; e), f) $CaCl_2$ and $FeCl_2$ in experiment A.

Figure 3: Peak phase frequency versus pH for all experiments (left axis); Fe^{2+} adsorption (right axis; Vikesland and Valentine (2002) and references therein). $CaCl_2$ data shown for experiments (A) and (B). Symbols represent effluent pH; error bars represent difference between influent and effluent pH. Note adsorption will vary with available surface area, solution chemistry and mineral purity; shaded area shows range published for Fe (oxyhydr)oxides, including magnetite (dashed line).

Figure 4: Example Cole-Cole model fits for $FeCl_2$ data, Solid symbols are phase data, open symbols are resistivity magnitude. Solid lines are model fits to the data for 0.1-94 Hz, dashed lines are extrapolations of these fits to 1000 Hz. Note that the Cole-Cole parameters for these fits are given in Table 1.

Figure 5: Conceptual model of magnetite response in SIP experiments: a) pH~4, Me^{2+} represents Ca^{2+}, Ni^{2+} or Fe^{2+}, magnetite surface is positively charged $>FeOH_2^{+1/2}$ b) pH 5 - 8, magnetite surface has increasing amount of $>FeOH^{-1/2}$ functional groups and progressive Fe^{2+} adsorption; charge transfer reactions (1) and (2) with charge transport through magnetite shown schematically, see text for details. Note that EDL thickness is vastly exaggerated, and magnetite particles shown as spheres, for illustration purposes; E represents applied electrical field that induces charge excess and deficit in magnetite lattice shown by - and + symbols. Adapted from Slater et al. (2005).

Table 1: Summary of the Cole-Cole parameters from the modeled fits to the SIP spectra for the different pore fluids from experiments A and B: ρ_0 is the DC resistivity, m is the chargeability (dimensionless), τ is the mean relaxation time, c is a shape exponent (dimensionless), m_n is the chargeability normalized to ρ_0,

and τ_n is the mean relaxation time normalized to ρ_0. The two specific pH fits for $FeCl_2$ correspond to the examples shown in Figure 4.

	ρ_0 (Ωm)	m x 10^{-3}	τ (msecs)	c	m_n x 10^{-3} (S/m)	τ_n (secs S/m x 10^{-6})
$CaCl_2$ (A)	74.6-79.6	95.9-98.3	1.94-2.14	0.690-0.707	1.25-1.29	24.4-27.7
$CaCl_2$ (B)	80.4-81.3	99.8-103	2.26-2.45	0.695-0.703	1.23-1.27	26.7-30.4
$NiCl_2$	83.4-85.5	97.2-101	2.26-2.56	0.700-0.713	1.15-1.19	26.5-30.7
$FeCl_2$	77.7-81.9	82.7-97.9	3.05-51.9	0.578-0.729	1.03-1.21	37.9-634
$FeCl_2$ (pH 4.7)	81.6	90.5	3.72	0.670	1.11	45.6
$FeCl_2$ (pH 6.3)	81.4	94.0	20.0	0.589	1.16	246

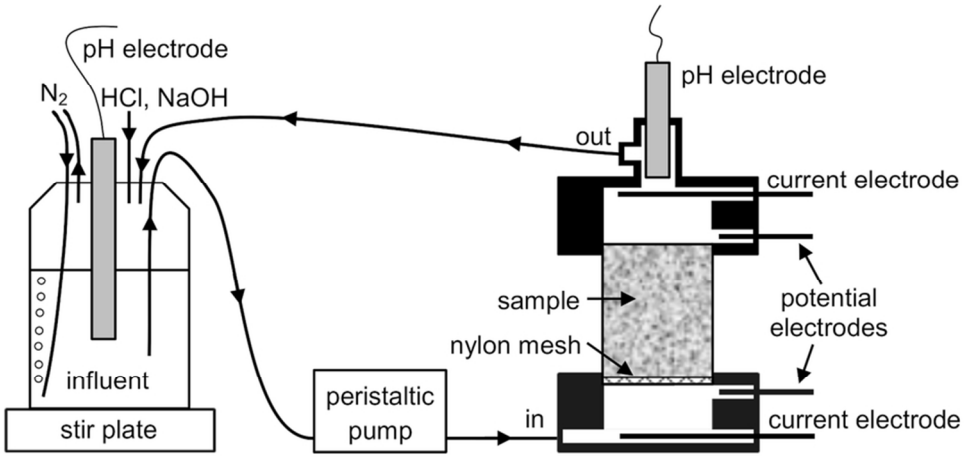

Schematic of laboratory apparatus (not to scale)
82x40mm (300 x 300 DPI)

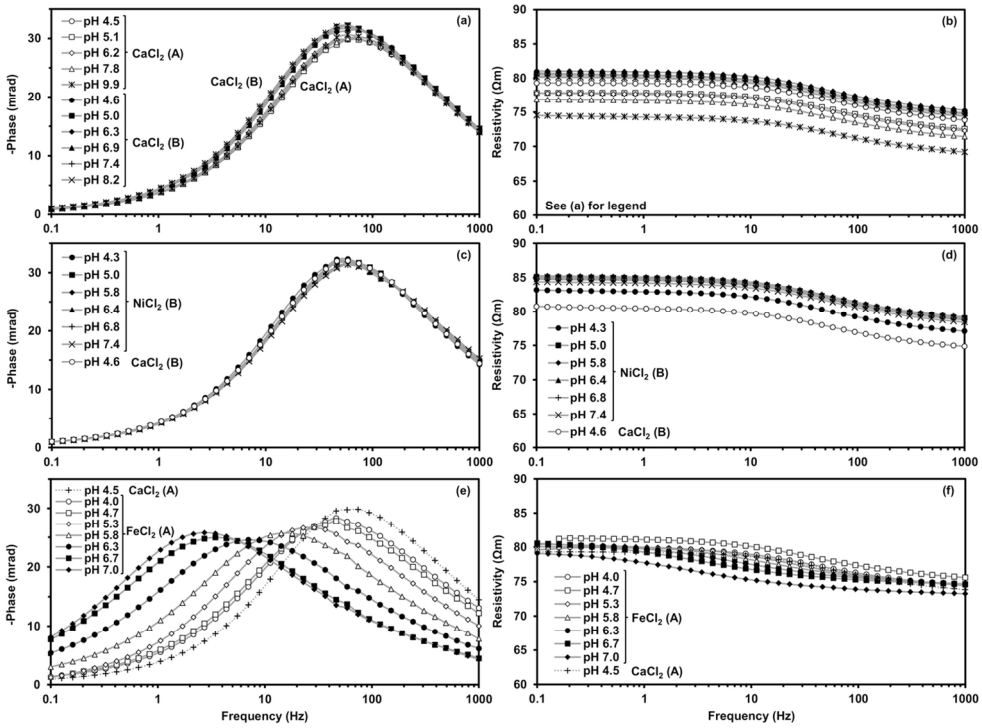

Spectral induced polarization data from 5 % magnetite in quartz sand experiments. a), b) phase and resistivity magnitude respectively for CaCl2 pore fluid in experiments A and B; c), d) NiCl2 and CaCl2 in experiment B; e), f) CaCl2 and FeCl2 in experiment A.
125x93mm (300 x 300 DPI)

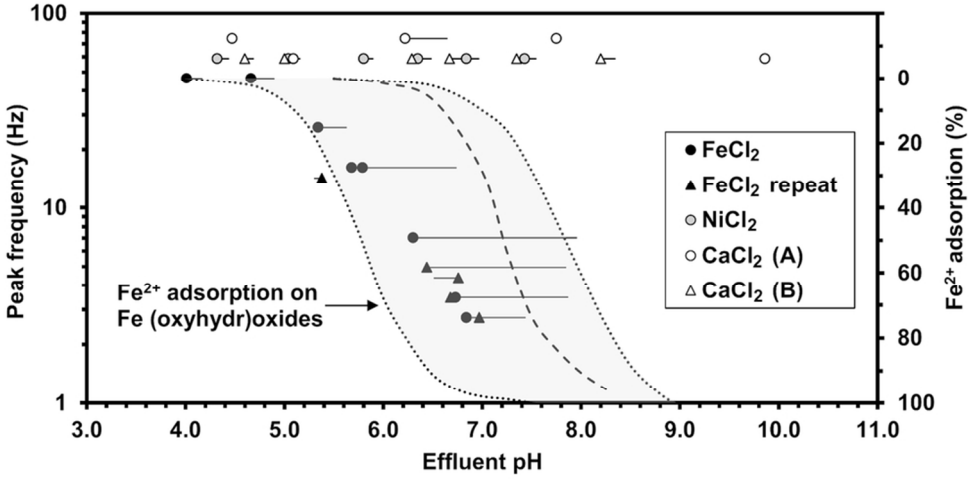

Peak phase frequency versus pH for all experiments (left axis); Fe2+ adsorption (right axis; Vikesland and Valentine (2002) and references therein). CaCl2 data shown for experiments (A) and (B). Symbols represent effluent pH; error bars represent difference between influent and effluent pH. Note adsorption will vary with available surface area, solution chemistry and mineral purity; shaded area shows range published for Fe (oxyhydr)oxides, including magnetite (dashed line).
86x44mm (300 x 300 DPI)

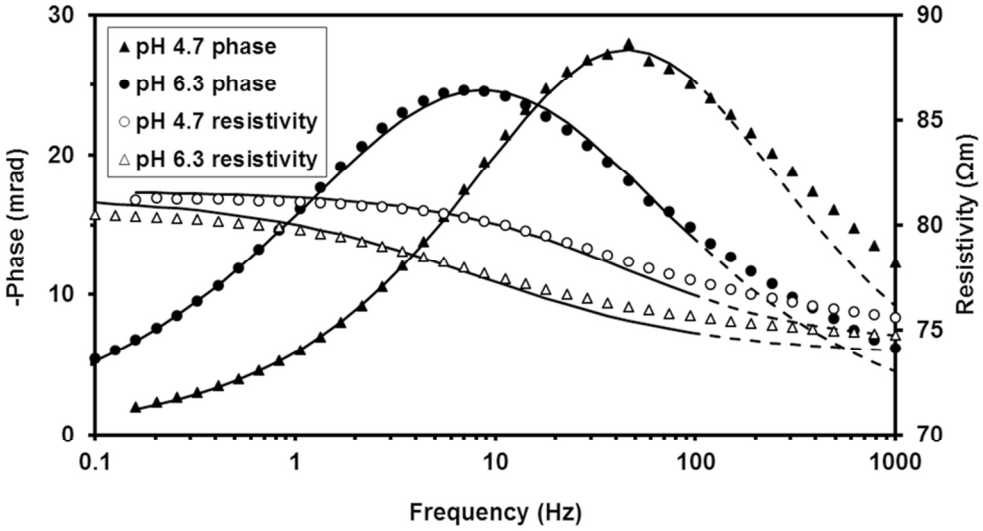

: Example Cole-Cole model fits for FeCl2 data, Solid symbols are phase data, open symbols are resistivity magnitude. Solid lines are model fits to the data for 0.1-94 Hz, dashed lines are extrapolations of these fits to 1000 Hz. Note that the Cole-Cole parameters for these fits are given in Table 1.
91x49mm (300 x 300 DPI)

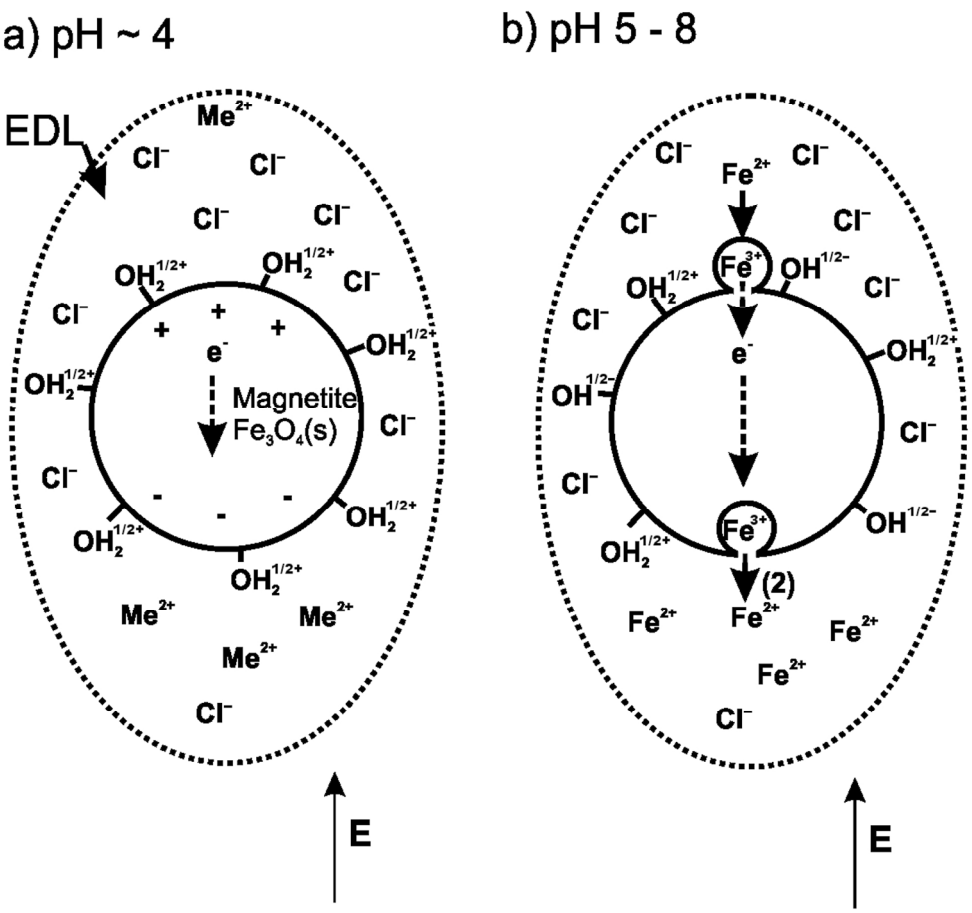

Conceptual model of magnetite response in SIP experiments: a) pH~4, Me2+ represents Ca2+, Ni2+ or Fe2+, magnetite surface is positively charged >FeOH2+1/2 b) pH 5 - 8, magnetite surface has increasing amount of >FeOH-1/2 functional groups and progressive Fe2+ adsorption; charge transfer reactions (1) and (2) with charge transport through magnetite shown schematically, see text for details. Note that EDL thickness is vastly exaggerated, and magnetite particles shown as spheres, for illustration purposes; E represents applied electrical field that induces charge excess and deficit in magnetite lattice shown by - and + symbols. Adapted from Slater et al. (2005).
169x153mm (300 x 300 DPI)